International Journal of Heat and Mass Transfer xxx (xxxx) xxx

Contents lists available at ScienceDirect

International Journal of Heat and Mass Transfer

journal homepage: www.elsevier.com/locate/hmt

Testing a simple Leeś disc method for estimating throuh-plane thermal conductivity of polymeric ion-exchange membranes

V.M. Barragán[a,*], J.C. Maroto[b,c], E. Pastuschuk[a], S. Muñoz[a]

[a] Department of Structure of Matter, Thermal Physics and Electronics, Complutense University of Madrid, Spain
[b] Department of Electronics, Automation and Communications, Comillas Pontifical University, Madrid, Spain
[c] Department of Science, Computing & Technology, Universidad Europea de Madrid, Spain

ARTICLE INFO

Article history:
Received 16 September 2021
Revised 5 November 2021
Accepted 20 November 2021
Available online xxx

Keywords:
Ion-exchange membranes
Thermal conductivity
Leeś disc
Polymer

ABSTRACT

Thermal conductivity of a material is a critical parameter for using it in non-isothermal applications. The new emphasis on using ion-exchange membranes as thermoelectric materials makes necessary to study the relation between thermal and structure properties. Here, through-plane thermal conductivity of different polymeric ion-exchange membranes was measured by a rapid experimental method using a simple Leeś Disc apparatus. Membranes with different structures and thicknesses in the interval 25–700 micrometers were analysed with the aim of testing the feasibility of the method in this kind of samples. Thermal conductivity of the investigated membranes was found to vary from as low as 0.03 up to as high as 0.41 W $K^{-1}m^{-1}$, depending on the type of membrane. Membranes with reinforcement in their structure presented lower values of the through-plane thermal conductivity. Although the thermal conductivity mainly depended on the composition of the membrane matrix, larger thermal resistances were estimated, in general, for membranes with higher density and thickness. No significant influence of the membrane ion-exchange capacity was observed for homogeneous and reinforced membranes, but a positive correlation was observed for heterogeneous membranes. The results obtained for homogeneous Nafion membranes were compared with values given in the literature for these same membranes, finding a good agreement. A thickness-dependent thermal conductivity was estimated for these membranes, suggesting that a size effect may play an important role in this kind of membranes. Despite its simplicity, the method allows to make a good estimation for the value of the through-plane thermal conductivity of polymeric ion-exchange membranes.

1. Introduction

Polymeric ion-exchange membranes are used in numerous applications based on electro-membrane processes. In these applications, transport numbers or ionic conductivity of the membranes are relevant parameters, and they have been widely studied in the literature. Even though large gradients may originate in the membrane systems, they have been neglected in literature so far and most of the transport processes are considered operating in isothermal conditions. Probably, that is one of the reasons why thermal conductivity of ion-exchange membranes has been little studied compared to other membranes properties. However, thermal conductivity of materials is an important issue in processes where a temperature gradient exists. Knowing thermal conductivity values of the involved materials is crucial when modeling the temperature distribution inside a non-isothermal system.

The use of membrane technology in energy conversion, such as fuel cells [1], reverse electrodialysis [2] or thermoelectricity [3] has increased the interest in the thermal properties of ion-exchange membranes. Thermal management is critical to the performance of these applications. In a fuel cell, a temperature distribution can be originated affecting the performance of the process, but until relatively recently, little attention has been paid to the thermal properties of fuel cell materials components [4,5,6]. It was probed that thermoelectric contributions to the cell potential can improve the cell performance in the otherwise isothermal reverse electrodialysis cell [7]. Thermoelectric properties are of interest to harvest useable electrical power from waste heat. The idea of using ion-exchange material for thermoelectric energy conversion purposes have been recently considered [3,7,8,9]. Nonetheless, regarding ion-exchange membranes, results have been basically referred

* Corresponding author.
E-mail address: vmabarra@ucm.es (V.M. Barragán).

https://doi.org/10.1016/j.ijheatmasstransfer.2021.122295

Table 1
Commercial polymeric ion-exchange membranes used in this work. (CEM: cation-exchange, AEM: anion-exchange).

Manufacturer	Name	Short Name	Structure	Reinforcement	Type
DuPont	Nafion N111	N111	homogeneous	Non	CEM
	Nafion N1135	N1135		Non	CEM
	Nafion N115	N115		Non	CEM
	Nafion N117	N117		Non	CEM
	Nafion N1110	N1110		Non	CEM
	Nafion N324	N324		PTFE	CEM
MEGA a.c.	Ralex CMHPES	RXCPES	heterogeneous	Polyester	CEM
	Ralex AMHPES	RXAPES		Polyester	AEM
	Ralex CMHPP	RXCPP		Polypropylene	CEM
	Ralex AMHPP	RXAPP		Polypropylene	AEM
ASTOM	Neosepta CMX	CMX	homogeneous	PVC	CEM
	Neosepta AMX	AMX		PVC	AEM
Ion Power	Ionics CR65-CZL-412	CR65	heterogeneous	Acrylic	CEM
	Ionics CR67-HMR-412	CR67		Polyacrylonitrile	CEM
AGC	Selemion CSO	CSO	homogeneous	PVC	CEM
GEFC	GEFC10	GEFC10	homogeneous	Non	CEM
Shchekinoazot	MK-40	MK40	heterogeneous	polyamide	CEM

to Nafion membranes in relation to its use as electrolyte in fuel cells [4,5,9,10,11] or in water electrolyzers [12].

Thermal conductivity is one of the key parameters if there exists temperature gradient in the systems. Thermogalvanic and thermoelectric material are characterized by the figure of merit ZT defined by [7,13]:

$$ZT = \frac{\eta_S{}^2 \sigma}{\kappa} T \tag{1}$$

where η_S is the Seebeck coefficient, σ and κ are, respectively, the electric and thermal conductivities of the material, and T is the absolute temperature. In such applications, ion-exchange membranes with large ionic conductivity but low thermal conductivity would be desirable. Thus, information on thermal conductivity of ion-exchange membranes, as well as on its relationship with other relevant membrane properties would be welcome.

Although efforts have been made to determine the thermal conductivity of polymers [13–18], many intrinsic and experimental parameters influence the resulting thermal conductivity of the material [17]. The thermal conductivity of a polymeric ion-exchange membrane depends on the polymer matrix, but also on the type of thermally conductive fillers, the existence of reinforcement on the structure, etc. Due to the almost infinite number of possible material compositions, it would be very important to estimate the properties of one candidate prior to a more precise study for using it in a given technology.

The methods for measuring thermal conductivity are generally classified in two regimes, permanent (steady state) and transient [19], and different approaches can be used [4,5,9–11,20–24]. The large of existing methods for the characterization of thermophysical properties shows that there is no single solution for all problem. So having a simple method to give a first estimation of thermal conductivity is also an important issue.

Leeś disc is a simple apparatus designed and utilised to measure conductivity of insulating materials. Leeś disc method has been used to investigate thermal conductivity of different kind of materials [25–27] but, to the best of our knowledge, it has not been used to measure thermal conductivity of ion-exchange membranes. The purpose of this work is to test the feasibility of the method to estimate through-plane thermal conductivity of thin polymeric ion-exchange membranes typically used in electromembrane-based applications and to analyse the influence of different membrane structural properties on their through-plane thermal conductivity.

2. Experimental

2.1. Ion-exchange membranes

Seventeen commercial polymeric ion-exchange membranes with different properties were tested in this work. They are presented in Table 1. Heterogeneous and homogeneous, anionic and cationic, and with different density membranes were used to the purpose of analysing the influence of these characteristics in the obtained results.

Nafion (N111, N1135, N115, N117, N1110) membranes are homogeneous non- reinforced membranes consisting of a polytetrafluoroethylene backbone and long fluorovinyl ether pendant side chains regularly spaced, terminated by a sulfonate acid group, with an equivalent weight (EW) of 1100 g/eq. There are no cross-links between the polymers. Nafion N324 membrane is a Teflon fabric reinforced membrane. It is a perfluorosulfonic acid cation-exchange membrane combining outstanding chemical resistance with strong polytetrafluoroethylene fiber reinforcement. Ionics (CR65, CR67) membranes are cation-selective membranes comprising cross-linked sulfonated copolymers of vinyl compounds. The membranes are homogeneous films, cast in sheet form on synthetic reinforcing fabrics. Modacrylic polymer (copolymer of vinyl chloride and acrylonitrile) or acrylic polymer are the fabrics most commonly used. Neosepta (CMX, AMX) are reinforced homogeneous membranes made by the paste method containing a reinforcing inert mesh. CMX cation membrane is a composite prepared on the base of polystyrene and divinylbenzene and reinforced with polyvinylchloride. The ionic fixed sites are sulfonic acid groups. AMX anion membrane is composed of styrene divinylbenzene copolymers with tri-alkyl ammonium fixed charge groups. MK-40 membrane is a sulphonic polystyrene divinylbenzene membrane of heterogeneous-type prepared by the inclusion of a finely ground ion-exchange resin in a polyethylene binder. It is made by hot rolling of low-pressure polyethylene, PE (used as a binder), with KU-2 ion-exchange resin powder. The size of polyethylene and ion-exchange resin particles is in the range from 5 to 50 micrometers. Reinforcing nylon mesh (where the diameter of filaments is of 30–50 microns) is introduced by hot pressing. GEFC10 membrane has a perfluorinated backbone and sulfonate side chains similar to Nafion membrane, but with a lower equivalent weight of 1000 g/eq. Selemion CSO is a monovalent selective cation exchange membrane that contains a thin polyethyleneimine (PEI) anion exchange layer. Heterogeneous Ralex membranes (RXCPES, RXAPES, RXCPP, RXAPP) are composites formed from ion-exchange resins with polyethylene basic binder and a reinforcing material. In RX-

Table 2
Thickness (d) and density (ρ) of the polymeric ion-exchange membranes tested in this work. Basic weight for non-reinforced Nafion membranes is also indicated.

Membrane	Thickness,d (10^{-6} m)	Density,ρ (kg m^{-3})	Basic Weight *(10^{-3} kg m^{-2})
N111	25	2000	50
N1135	89	1985	190
N115	131	2000	250
N117	186	1980	360
N1110	254	1985	500
N324	271	1550	–
RXCPES	431	817	–
RXAPES	454	945	–
RXCPP	422	1120	–
RXAPP	422	917	–
CMX	151	1000	–
AMX	129	900	–
CR65	612	877	–
CR67	685	833	–
CSO	81	1310	–
GEFC10	260	2150	–
MK40	450	1120	–

*Given by the manufacturer.

CPES (cationic) and RXAPES (anionic), the reinforcing material is a polyester fitting fabric. For RXCPP (cationic) and RXAPP (anionic) the reinforcing material is polypropylene.

Membrane thickness was measured with a PCE-THM-20 material thickness meter with resolution 0.0002 mm. Final value of membrane thickness was obtained by averaging the results of at least ten measurements made at different points of the sample under study. The maximum standard error was always lower than 0.001 mm. The obtained values are shown in Table 2, together with the values of the density determined for each membrane. This last parameter was obtained by measuring the area and the mass of a corresponding membrane sample.

2.2. Experimental device

Through-plane thermal conductivity of the studied membranes was estimated by using the Leeś disk method. Fig. 1 shows a sketch of the experimental device used in this work. It consisted of two brass (red or yellow) discs of cylindrical shape. The discs were placed on top of each other with the membrane sample, whose conductivity was to be determined, placed in the middle.

The top metal disc (metal chest) was hollow at its top to allow the steam in and out, while the bottom disc was a thinner solid metal piece. A hole was made in each disc, close to the surface in contact with the tested sample, where a Pt100 sensor was placed

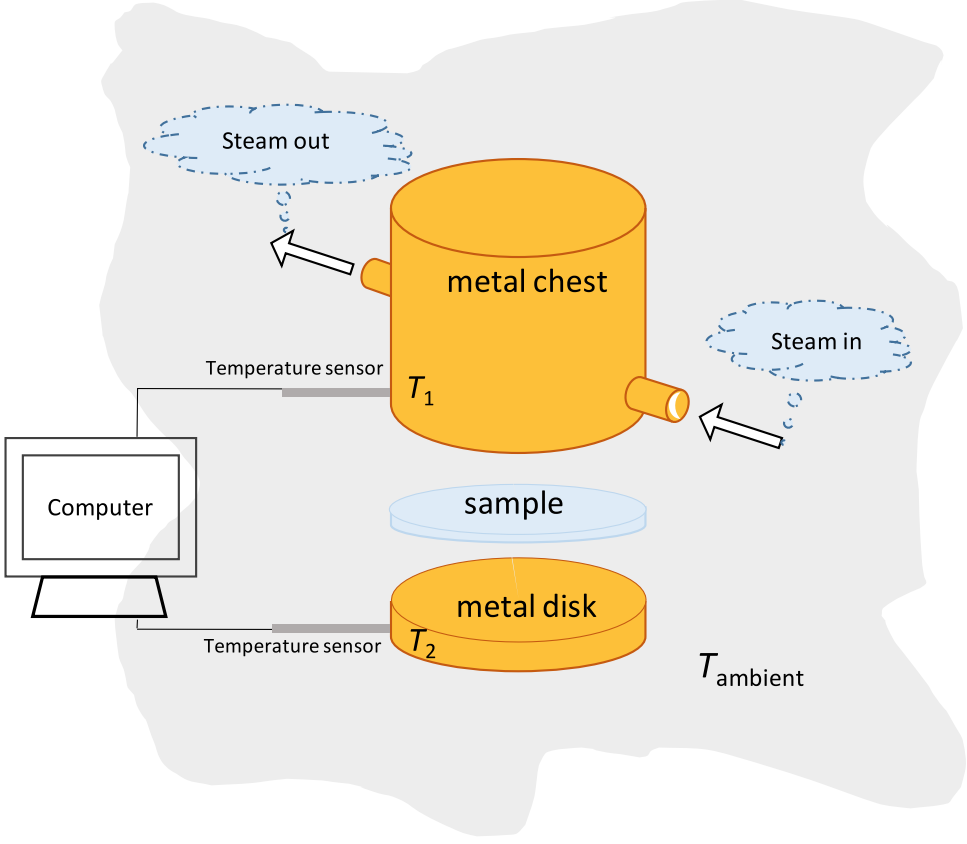

Fig. 1. Sketch of the experimental device used in this work.

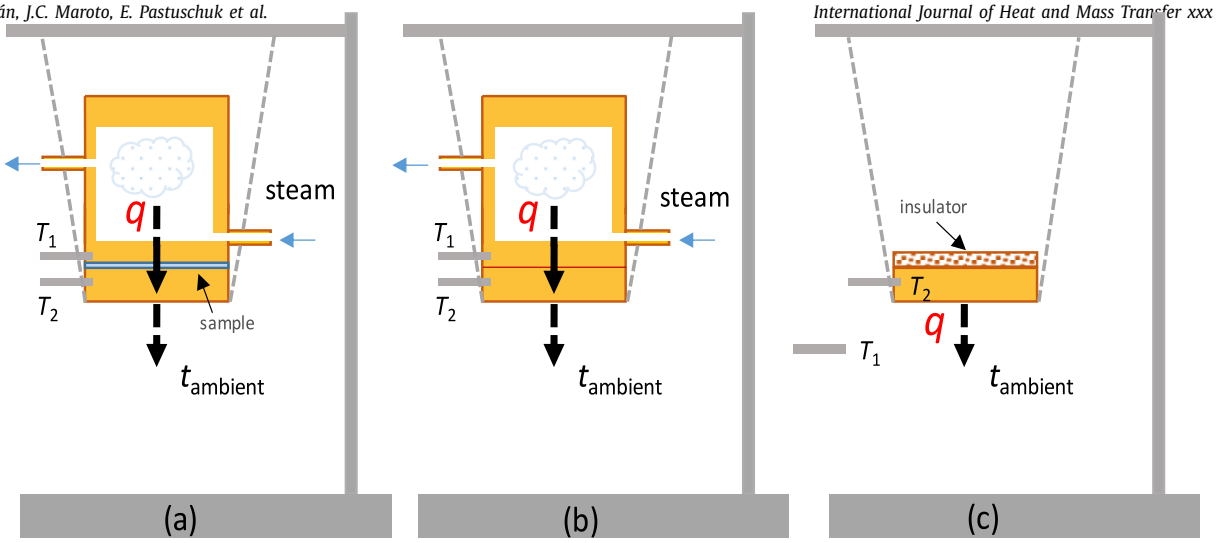

Fig. 2. Sketch of the three steps of the measurement process. (a) Step 1: Stationary state; (b) Step 2: lower metal disc heating; (c) Step 3: lower metal disc cooling.

Table 3
Values of relevant parameters for the experimental devices.

Diameter of discs (10^{-3} m)	98.44 ± 0.02
Thickness of bottom disc (10^{-3} m)	12.00 ± 0.02
Mass of bottom disc $\boldsymbol{m}$ (10^{-3} kg)	
Red Brass	788.50 ± 0.05
Yellow Brass	755.0 ± 0.1
Mass of top disc (10^{-3} kg)	
Red Brass	1304.8 ± 0.1
Yellow Brass	1305.9 ± 0.1
Specific heat, $\boldsymbol{c}$ (J kg^{-1}K^{-1})	
Red Brass	380 ± 1
Yellow Brass	380 ± 1

in to measure the temperatures T_1 and T_2 of the discs. These temperatures were recorded by a computer.

The experiment consisted of three steps. First (Step 1), the sample was placed between the two discs and steam was made circulating through the top metal chest. Steam was produced by boiling water. The temperatures T_1 and T_2 were recorded until the steady state was reached when both temperatures kept constant (Fig. 2a). The sample was then removed and both metal discs were kept in contact until they reached approximately the same temperature (Step 2) (Fig. 2b). Afterwards (Step 3), the top metal disc was removed, and a sample of an insulating material (cork) was placed over the bottom disc to ensure that their cooling occurs under the same conditions as in Step 2. In this configuration (Fig. 2c), the bottom disc was cooled to room temperature, measuring its temperature during the cooling process. The sensor T_1 was placed nearby to measure ambient temperature during the cooling process.

The membrane samples were machined approximately with the same diameter of the discs (around 9 cm). Table 3 shows values for relevant parameters of the device.

2.3. Theoretical background

Consider steady one-dimensional heat transfer through a plane wall consisting of three layers of different materials with thickness l_1, d and l_2, and thermal conductivities κ_1, κ and κ_3, respectively (Fig. 3). The external surface of the wall$_1$ is in contact with a fluid at constant temperature $T_{\infty w}$, and the external surface of wall$_2$ is in contact with a fluid at constant temperature $T_{\infty a}$. h_1 and h_2 represent the heat transfer coefficients for the convection heat transfer between the fluids and the solid external surface of area A of

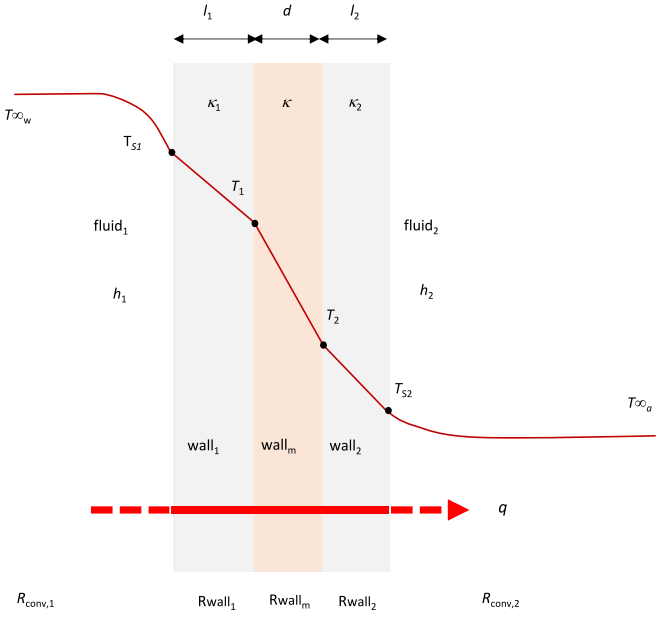

Fig. 3. Stationary temperature profile through a three layers plane wall subjected to convection on both external sides.

the walls$_1$ and wall$_2$, respectively. Although the heat transfers will occur in both perpendicular and parallel directions to the layers surface, if the thickness of the wall is small, the temperature gradient in that direction will be large. Moreover, if the fluid temperatures inside and outside remain constant, then heat transfer through the wall can be modelled as unidirectional and can be expressed as $T(z)$ [28]. When the area A and the rate of conduction heat transfer are constant, the temperature through the wall varies linearly with z. That is, the temperature distribution in the wall under steady conditions would be a straight line. The thermal resistance concept can be used to determine the rate of the steady heat transfer through the composite wall.

Despite the complexity of convection, the rate of convection heat transfer through the wall$_1$ and wall$_2$ are observed to be proportional to the temperature difference and is conveniently expressed by Newtonś law of cooling as:

$$Q_{\text{conv}} = q_{\text{conv}}A = -h_1A(T_{s1} - T_{\infty w}) = -h_2A(T_{\infty a} - T_{s2}) \tag{2}$$

The conduction heat flow, q, due to a temperature gradient, ∇T, can be expressed by the Fourier law:

$$\overrightarrow{q}_{\text{cond}} = -\overline{\kappa}\nabla T \tag{3}$$

where $\overline{\kappa}$ is the thermal conductivity coefficient tensor. If a homogeneous plane body is considered, we can consider a unidimensional heat transfer and according to Eq. (3), in the stationary state, the rate of heat transfer, Q, transmitted by conduction through the different layers of the wall can be expressed by:

$$Q_{\text{cond}} = q_{cond}A = -\kappa_1 A\frac{(T_1 - T_{s1})}{l_1} = -\kappa A\frac{(T_2 - T_1)}{d} = -\kappa_2 A\frac{(T_{s2} - T_2)}{l_2} \tag{4}$$

where T_i and T_j represent the corresponding temperatures over the two surfaces of each layer, and k_i indicates the corresponding thermal coefficient in the considered direction.

Using the analogy between thermal and electrical resistance concepts, we can rearrange Eqs. (2) and (4) as a function of the thermal resistances R_{conv} and R_{cond}, corresponding respectively to convection and conduction heat transfers, defined as:

$$Q_{\text{conv}} = \frac{(T_\infty - T)}{\frac{1}{hA}} = \frac{(T_\infty - T)}{R_{\text{conv}}} \tag{5}$$

$$Q_{\text{cond}} = \frac{(T_1 - T_2)}{\frac{d}{\kappa A}} = \frac{(T_1 - T_2)}{R_{\text{cond}}} \tag{6}$$

Under steady conditions, the rate of the heat transfer must be the same through all the walls and, according to Eqs. (5) and (6), for the considered system (Fig. 3), we have:

$$Q_{\text{cond}} = Q_{\text{conv}} = \frac{(T_{\infty w} - T_{\infty a})}{R_{\text{conv},1} + R_{\text{wall}_1} + R_{\text{wall}_m} + R_{\text{wall}_2} + R_{\text{conv},2}} \tag{7}$$

where:

$$R_{\text{conv},1} = \frac{1}{h_1 A};\quad R_{\text{wall}_1} = \frac{l_1}{\kappa_1 A};\quad R_{\text{wall}_m} = \frac{d}{\kappa A};$$
$$R_{\text{wall}_2} = \frac{l_2}{\kappa_2 A};\quad R_{\text{conv},2} = \frac{1}{h_2 A} \tag{8}$$

Or:

$$Q = \frac{(T_{\infty w} - T_{s1})}{R_{\text{conv},1}} = \frac{(T_{s1} - T_1)}{\frac{l_1}{\kappa_1 A}} = \frac{(T_1 - T_2)}{\frac{d}{\kappa A}}$$
$$= \frac{(T_2 - T_{s2})}{\frac{l_2}{\kappa_2 A}} = \frac{(T_{s2} - T_{\infty a})}{R_{\text{conv},2}} \tag{9}$$

On the other hand, the amount of heat emitted by a body of mass m and specific heat c, at temperature T_s, cooling can be expressed by:

$$Q = mc\left(\frac{dT}{dt}\right)_{Ts} \tag{10}$$

where t indicates time.

In the considered case, if T_{s2} over the external surface of wall$_2$ is kept constant, it is necessary that the stationary Q is the same in Eqs. (9) and (10). Thus:

$$\kappa = \frac{mcd}{A(T_1 - T_2)}\left(\frac{dT}{dt}\right)_{Ts_2} \tag{11}$$

where m is the mass of the wall$_2$. Supposing that wall$_2$ is cooling in contact with fluid$_2$, air in this case, according to the Newtonś law of cooling (Eq. 2), its temperature will decrease in time with an exponential dependence:

$$T = T_{\infty a} + \alpha \exp(-\beta t) \tag{12}$$

where β and α are parameters, related to the air heat transfer coefficient and temperatures of cooling surface and air. From Eq. (12) the rate of cooling can be expressed as

$$\left(\frac{dT}{dt}\right)_{Ts_2} = -\beta(T_{s2} - T_{\infty a}) \tag{13}$$

And from Eqs. (11) and (13), thermal conductivity coefficient of wall can be estimated as:

$$\kappa = \frac{mcd\beta(T_{s2} - T_{\infty a})}{A(T_1 - T_2)} \tag{14}$$

If the emissivity of the external surface of wall$_2$ is not null, a radiation heat transfer also occurs simultaneously to the convection heat transfer during the cooling of the surface. For one-dimensional heat transfer, according to the Stefan- Boltzmann law, the heat transfer between the surface, at temperature T_{s2} and the surroundings, at temperature T_0, can be expressed as:

$$Q_{\text{rad}} = \sigma\varepsilon A\left(T_{s2}^4 - T_0^4\right) \tag{15}$$

where ε is the emissivity of the boundary surface and σ is the Stefan-Boltzmann constant. This expression can also be expressed in a linear form by an analogous expression to Eq. (2) introducing a named radiation coefficient h_r, which depends on the temperature, as:

$$Q_{\text{rad}} = h_r A(T_{s2} - T_0) \tag{16}$$

In the studied case, the amount of heat emitted by the surface will be due to a combination of both processes, and the surrounding temperature is also the air temperature $T_{\infty a}$. The use of h_r allows to express the combined heat flux from the cooling surface by means of a combined heat transfer coefficient h_{air} that includes the effects of both convection and radiation. Thus, we can rewrite Eq. (2) as [29]:

$$Q_{\text{conv+rad}} = -h_{\text{air}}A(T_{\infty a} - T_{s2}) = -(h_2 + h_r)A(T_{\infty a} - T_{s2}) \tag{17}$$

where

$$h_r = \sigma\varepsilon\left(T_{\infty a}^2 + T_{s2}^2\right)(T_{\infty a} + T_{s2}) \tag{18}$$

Radiation is usually considered negligible relative to forced convection, but it is significant relative to conduction or natural convection, and β in Eq. (12) would be the parameter that considers both effects in the cooling process.

Eq. (14) can be used to estimate the thermal conductivity of the membrane sample. Wall$_1$ and wall$_2$ would be, respectively, the upper and bottom discs, and wall$_m$ corresponds to the membrane sample under test. As the surface of the discs is higher in comparison to their thickness, we can consider a unidimensional heat transfer problem similar to the one shown in Fig. 3. Taking into account that the thermal conductivity of brass is very high, the thermal resistance of the brass discs, corresponding to wall$_1$ and wall$_2$ in Fig. 3, will be negligible from Eq. (9), and thus the temperature is uniform through each disc, that is, $T_1 \sim T_{s1}$ and $T_2 \sim T_{s2}$. Considering the area for the cylindrical shape of the bottom disc, Eq. (14) can be expressed as:

$$\kappa = \frac{4mcd\beta(T_2 - T_{\infty a})}{\pi D^2(T_1 - T_2)} \tag{19}$$

In Eq. (19), temperatures T_1 and T_2 are experimentally determined in the step 1 of the experiments, β and $T_{\infty a}$ are estimated from the experimental results in the step 3 of the experiments, m and c are known parameters of the used device, and d and D are known for each tested membrane sample. The value of T_a should be close to the experimental value measured with sensor T_2 in the step 3 of the experiments.

According to the third term in Eq. (8), thermal resistance of the tested samples can be estimated, as:

$$R_m = \frac{4d}{\kappa\pi D^2} \tag{20}$$

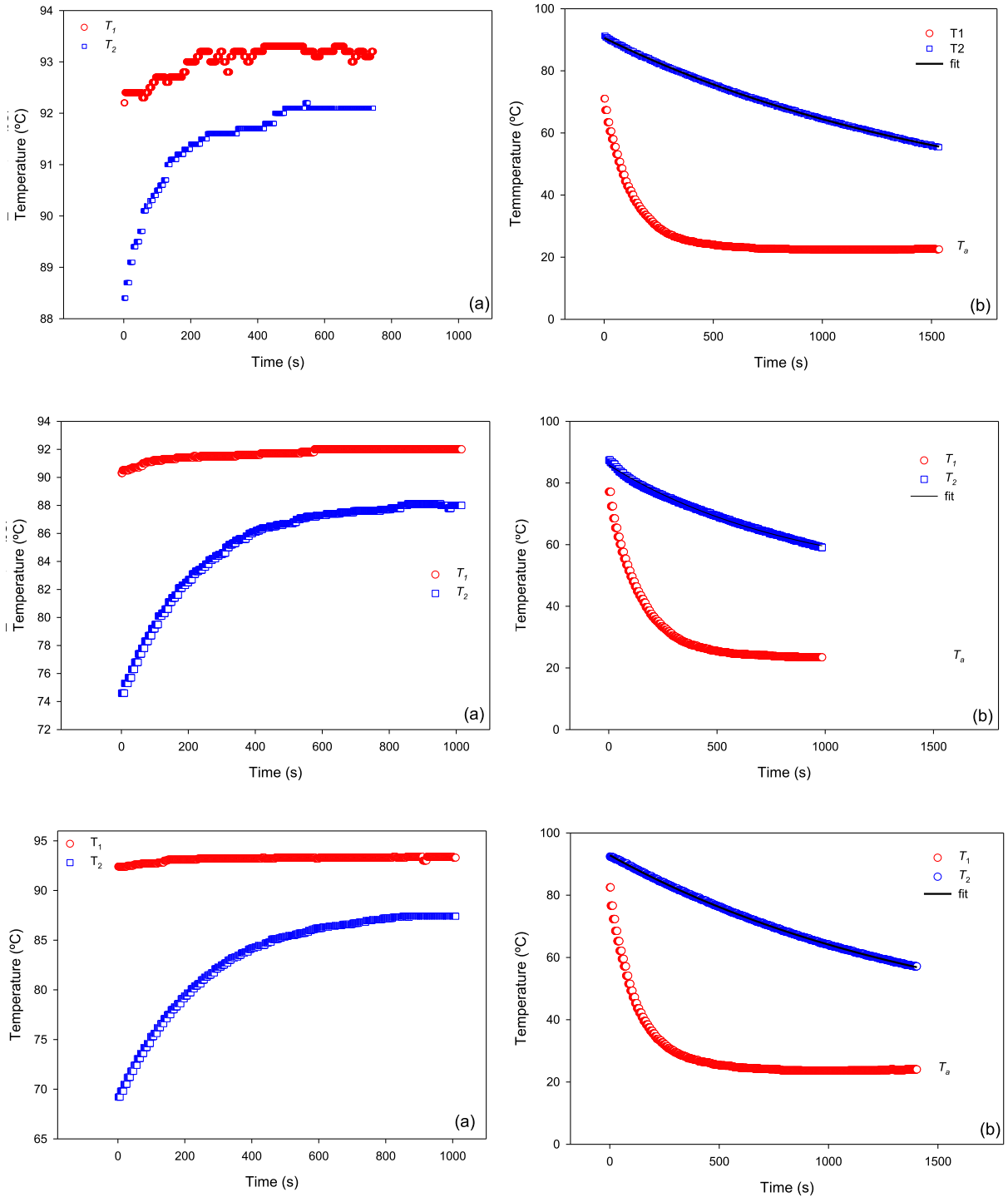

Fig. 4. Temperature-time curves for three of the studied cases. (a) Stationary (step 1); (b) Cooling (step 3). Top figures correspond to homogeneous NF117 membrane, middle figures to reinforced homogeneous CMX membrane, and bottom figures to heterogeneous CR67 membrane. T_1, T_2 and T_a represent, respectively, the temperatures of the top and bottom metal discs and the ambient temperature. Continuous lines in (b) are the fits to the experimental T_2 values to Eq. (12).

3. Results and conclusions

The procedure described in Section 2.2 was carried out for the different tested membranes. As examples, Fig. 4 shows temperatures T_1 and T_2 measured in the steps 1 and 3 as a function of time for three of the studied cases.

Similar profiles were obtained for the different tested membranes. In the step 1 (Fig. 4a), a stationary state was reached after a time that depends on the sample and the ambient temperature. In the step 3 (Fig. 4b), the temperature in the sensor T_2 decreased, and in the sensor T_1 reached the ambient temperature.

3.1. Temperatures of the stationary state

Temperatures T_1 and T_2 in the step 1 (Fig. 4a) were estimated from the average recorded temperature values once the steady

Table 4
Temperatures reached in top (T_1) and bottom (T_2) discs, the average value of both temperatures (T_{av}), and the temperature differences in the stationary state (Step 1) for each experiment.The temperature measurement error was ±0.1 K. The standard deviation was also lower than the measurement error.

Membrane	T_1 (°C)	T_2 (°C)	T_{av} (°C)	ΔT(K)
N111	93.7	92.6	93.2	1.1
N1135	93.8	92.8	93.3	1.0
N115	93.0	92.1	92.6	0.9
N117	93.2	92.1	92.7	1.1
N1110	93.2	92.2	92.7	1.0
N324	93.4	89.7	91.6	3.7
RXCPES	91.5	89.1	90.3	2.4
RXAPES	93.2	90.5	91.9	2.7
RXCPP	92.2	90.5	91.4	1.7
RXAPP	91.7	87.5	89.6	4.2
CMX	92.0	88.0	90.0	4.0
AMX	93.3	91.5	92.4	1.8
CR65	93.5	87.4	90.5	6.1
CR67	93.3	87.4	90.4	5.9
CSO	91.6	89.0	90.3	2.6
GEFC10	93.0	91.3	92.2	1.7
MK40	92.7	91.1	91.9	1.6

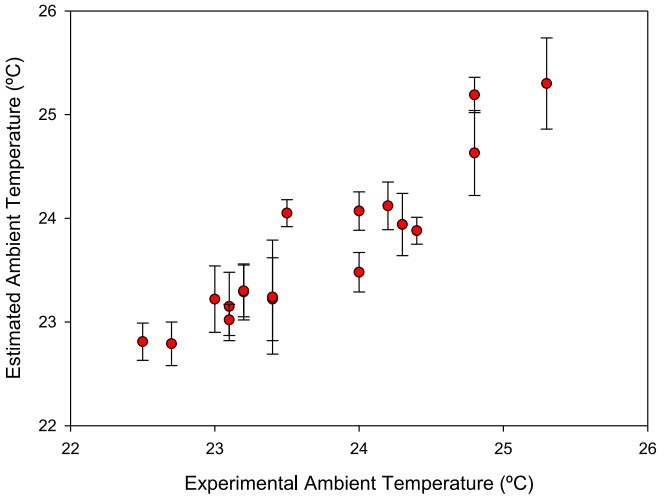

Fig. 5. Comparison between the values of the ambient temperature obtained experimentally and from the cooling curve.

state was reached. These values, the average value of both, as well as the difference between them, are shown in Table 4 for the different membrane samples tested in this work.

3.2. Cooling process

In the step 3, the lower disc was allowed to cool and its temperature was recorded during the process. The experimental data were fitted to Eq. (12). It allowed us to estimate the values of parameter β and the ambient temperature, T_a in each experiment. The results are shown in Table 5. The experimental value of the ambient temperature during the cooling process was also estimated from the average values recording by the sensor T_2 in the step 3. This value is also shown in Table 5. The correlation factor was higher than 0.99 in the most unfavourable case.

Fig. 5 compares experimental and estimated values for the ambient temperature. As it can be observed, the values predicted by the fits are in good agreement to the experimental values, the relative deviation being always less than 5% in the most unfavourable case.

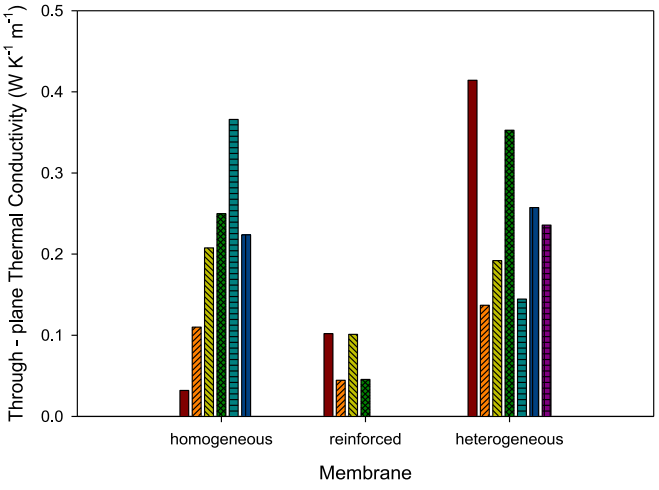

Fig. 6. Thermal conductivity for non-reinforced and reinforced homogeneous membranes, and heterogeneous membranes tested in this work.

3.3. Estimation of through-plane thermal conductivity

From data in Tables 3–5, the through-plane thermal conductivity of the tested membranes at the corresponding average temperature can be obtained from Eq. (19). The values are also shown in Table 5. Values varied between 0.03 and 0.41 $WK^{-1}m^{-1}$, depending on the membrane structure and composition, which agree with the thermal conductivity values of typical polymers. Thus, values of 0.27 and 0.35 $WK^{-1}m^{-1}$ are given, respectively, for polytetrafluoroethylene (PTFE), one of the basic components of Nafion membranes, and polyphenylsulfone (PPSU) at 25 °C [30]. Typical values for thermal conductivity of polystyrene, one of the components of CMX membrane, are between 0.030 and 0.040 $WK^{-1}m^{-1}$ [31], in agreement with the lower value 0.045 $WK^{-1}m^{-1}$ obtained for the thermal conductivity of this membrane. The highest value was obtained for the heterogeneous MK40 membrane. Although this membrane is also a sulphonic polystyrene divinylbenzene membrane, it has a polyethylene binder. The thermal conductivity of polyethylene is between 0.33–0.50 $WK^{-1}m^{-1}$, while the reinforced material for CMX membrane is polyvinylchloride with thermal conductivity of 0.13–0.29 $WK^{-1}m^{-1}$ [17], which could explain the higher thermal conductivity of MK40 membrane.

The values obtained for N115 and N117 are in agreement with the results found in the literature for Nafion membranes. Reported values in literature for Nafion membranes varied in the interval 0.1–0.25 $WK^{-1}m^{-1}$, depending on the used method [4,5,9,10,24,32].

Fig. 6 shows the values obtained for the thermal conductivity of the different membranes grouped according to their structure, homogeneous, reinforced or heterogeneous. As it can be observed, lower values were obtained, in general, for tested homogenous reinforced membranes.

Thermal conductivity values for ion-exchange membranes are scarce in the literature. Most of them refer to the Nafion membrane, but often the type of Nafion used is not specified and it is assumed that bulk properties of Nafion dont́ depend on the membrane thickness. Kandelwal and Mench [4] obtained 0.16 ± 0.03 $WK^{-1}m^{-1}$ for Nafion membrane at room temperature, finding a dependence with humidity and temperature. Burheim et al. [11] also showed that thermal conductivity of Nafion depended on the wet state of the membrane with value of 0.177 ± 0.008 $WK^{-1}m^{-1}$ in dried state. Joniken et al. [9] and Ahadi et al. [10] gave, respectively, values of 0.25 and 0.243 ± 0.007 $WK^{-1}m^{-1}$ for Nafion. Through-plane thermal con-

Table 5
Cooling curve parameters fitting, β and $T_{\infty a,}$ experimental ambient temperature, T_a, and thermal conductivity coefficient, κ, estimated for each tested membrane. The temperature measurement error was ±0.1 K. Standard deviations for β and κ are also shown.

Membrane	β (10^{-4} s^{-1})	$T_{\infty a}$ (°C)estimated	T_a (°C)measured	κ (W K^{-1} m^{-1})
N111	5.143 ± 0.025	23.9 ± 0.3	24.3	0.032 ± 0.004
N1135	4.640 ± 0.019	25.19 ± 0.17	24.8	0.110 ± 0.016
N115	5.12 ± 0.04	23.2 ± 0.3	23.0	0.21 ± 0.03
N117	4.938 ± 0.023	22.8 ± 0.18	22.5	0.25 ± 0.03
N1110	5. 413 ± 0.025	23.6 ± 0.4	24.8	0.37 ± 0.05
N324	4.951 ± 0.019	23.02 ± 0.15	23.1	0.102 ± 0.004
RXCPES	5.32 ± 0.05	25.3 ± 0.4	25.3	0.252 ± 0.016
RXAPES	5.439 ± 0.027	24.07 ± 0.19	24.0	0.236 ± 0.013
RXCPP	4.758 ± 0.024	22.79 ± 0.21	22.7	0.35 ± 0.03
RXAPP	5.143 ± 0.019	24.05 ± 0.13	23.5	0.141 ± 0.005
CMX	4.50 ± 0.07	23.3 ± 0.6	23.4	0.044 ± 0.002
AMX	5.20 ± 0.03	23.30 ± 0.25	23.2	0.099 ± 0.008
CR65	5.271 ± 0.026	23.48 ± 0.19	24.0	0.140 ± 0.004
CR67	5.26 ± 0.05	23.2 ± 0.4	24.2	0.159 ± 0.005
CSO	4.85 ± 0.04	23.29 ± 0.27	23.2	0.046 ± 0.003
GEFC10	5.15 ± 0.03	24.12 ± 0.23	24.2	0.224 ± 0.019
MK40	5.124 ± 0.04	23.1 ± 0.3	23.1	0.41 ± 0.04

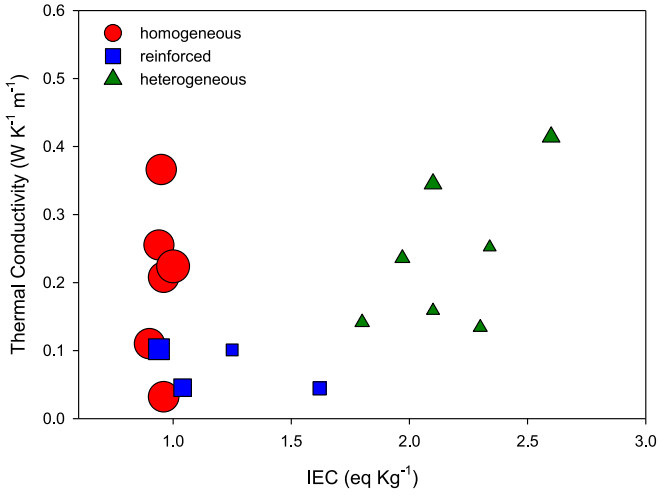

Fig. 7. Thermal conductivity as a function of the ion exchange capacity expressed in equivalent per mass of dry membrane. The size of symbols in the bubble plot is proportional to the membrane density.

ductivity as a function of temperature and water content were reported by Alhazmi et al. [6] for Nafion 115 membranes, obtaining values between 0.193 ± 0.018 and 0.13 ± 0.02 $WK^{-1}m^{-1}$, being this dependence a result of increasing the number of phonons at the high temperature for the polymers as Nafion material which is consideed as an insulating material [32]. Values of 0.22 and 0.25 $WK^{-1}m^{-1}$ were found for Nafion 115 and 117, respectively, using a finite element technique [24].

To analyse the influence of the charge group fixed in the membrane matrix, Fig. 7 represents the thermal conductivity as a function of the ion-exchange capacity of the membrane. No significant correlation was observed between both parameters for homogeneous and reinforced membranes.

A positive correlation was observed for heterogeneous membranes. Similar behavior was observed with amorphous polymers containing charged oxygen and nitrogen atoms [33]. However, the various membranes have different physical properties and this behavior could be due to the influence of the membrane density. It can see in Fig. 7 that heterogeneous membranes with higher ion-exchange capacity also correspond to the membranes with higher density. For reinforced membranes, it is observed that an increase of the ion-exchange capacity doesnt́ lead to an increase in the thermal conductivity. This is an important point to consider with respect to the use of charged polymers as thermoelectric material. For this application, both high ion-exchange capacity and low thermal conductivity are needed. Results presented in Fig. 7 would point that it is possible to increase IEC without increasing the thermal conductivity of the membrane.

Fig. 8 presents the values of thermal conductivity obtained in this work for the tested homogeneous Nafion membranes as a function of their thickness.

As can be observed, a linear relation is observed between thermal conductivity and thickness for the non-reinforced Nafion membranes. This is an anomalous result, because what would be expected is a thermal conductivity independent of the membrane. However, the lower conductivity of the thinner Nafion membranes is clear. A similar behavior was found by Slade et al. [34] for the ionic conductivity of the Nafion 1100 WE series of membranes. They concluded that the unexpected decrease in ionic conductivity of thin membranes could be related to their extrusion production process. Temperature and pressure would have a pronounced effect on the surface structure of the material resulting in a decrease of the membrane channel or an increase in the membrane tortuosity. A thickness-dependent thermal conductivity has been also found by Feng et al. [33] in amorphous polymers. They found that thermal conductivities of amorphous polymers can be further reduced below their bulk limit due to size effects. Tarkhanyan and Niarchos [35] also studied the reduction in the lattice thermal conductivity of porous materials due to size effect. The external reinforcement existing in the structure of the N324 membrane seems to decrease its thermal conductivity. The measured thickness for this membrane considers the external PTFE reinforcement in the membrane structure. According to the manufacturer, this membrane is composed by a main layer of 125 μm with a multifilament yarn, with a resulting fabric with 32% of open area and a less smooth surface than the rest of the tested Nafion membranes. A larger contribution of the contact resistances would be expected for this membrane, but these are not explicitly considered.

An additional experiment was carried out using two samples of MK40 membrane placed together in step 1. In this case, a temperature gap of 2.8 K was obtained, with an ambient temperature of 24 °C. The adjustable parameters $T_{\infty a}$ and β were, respectively, 23.99 °C and 5.163 × 10^{-4} s^{-1}, giving as result for the thermal conductivity of this membrane a value of 0.408 WK^{-1} m^{-1}, which is a relative difference from the value obtained using only one membrane sample of less than 2%. Thermal resistances for one and two MK40 samples can be estimated from Eq. (20), obtaining values of 0.153 and 0.292 KW^{-1}, respectively. Considering the linear depen-

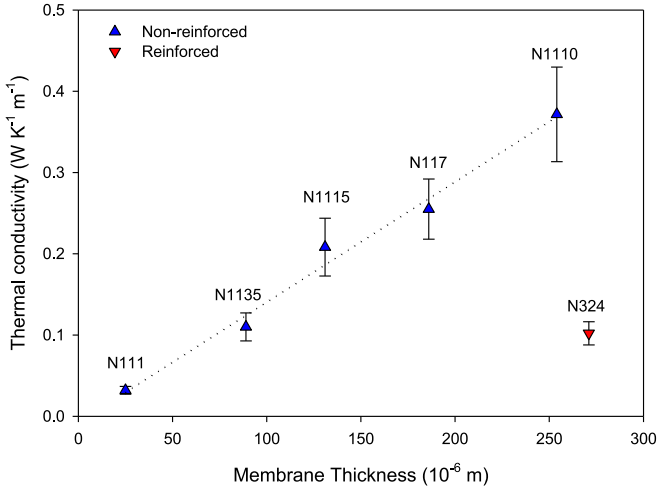

Fig. 8. Thermal conductivity as a function of the membrane thickness for the Nafion 1100 EW series of membranes tested.

dence between resistance and thickness of the membrane sample, the estimated contribution of the contact resistances would fall within the range of experimental error. This supports our idea that the contribution of the contact resistance to the estimated value for the thermal conductivity is within the range of experimental error, although it would be necessary to take them into account in order to obtain a more precise value. We have compared the thermal conductivity values obtained in this work with those obtained in [24] using a finite element technique with some of the same membranes used in this work. In that work, the contact resistance was taking into account. For all the compared membranes, the difference observed between the values obtained with both methods was within the experimental error.

Thermal resistances of the tested membranes, estimated from Eq. (20), are shown in Fig. 9 versus density and thickness of the membranes. Due to the different composition of the membranes, it is difficult to analyse the influence of thickness and density in the measured through-plane thermal conductivity. But the results presented in Fig. 9 show that, in general, denser homogeneous membranes showed lower thermal resistances. It should be noted, however, that in applications where the membrane is immersed in an aqueous electrolyte medium, the types of salt ions and membrane water content can also play an important role in the effective thermal conductivity value.

Considering the cooling convection processes over the external surface of the bottom metal disc, it is possible from Eqs. (10) and (17) to estimate the combined heat transfer coefficient in the cool-

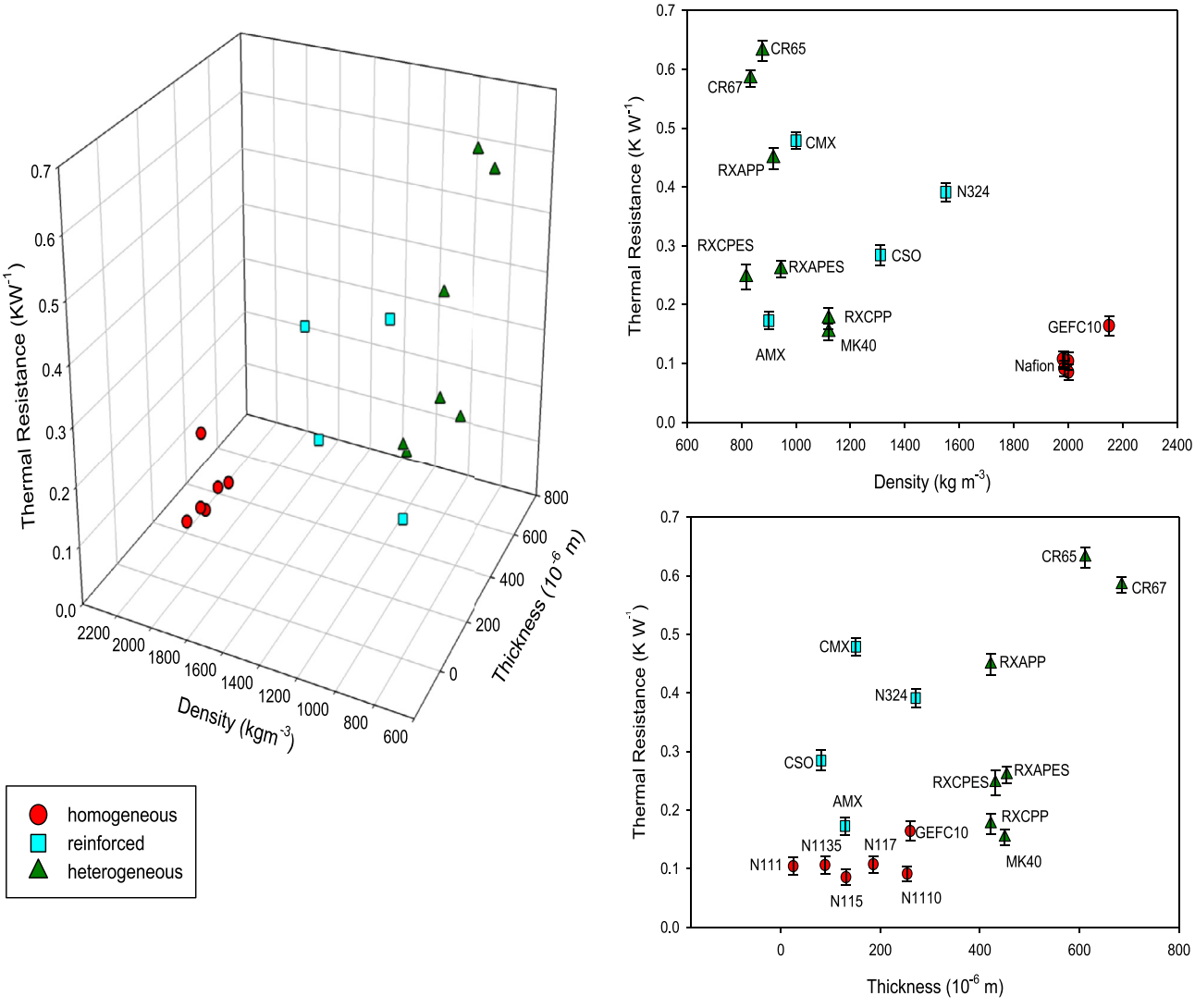

Fig. 9. Thermal resistance of the tested membranes as a function of density and of thickness.

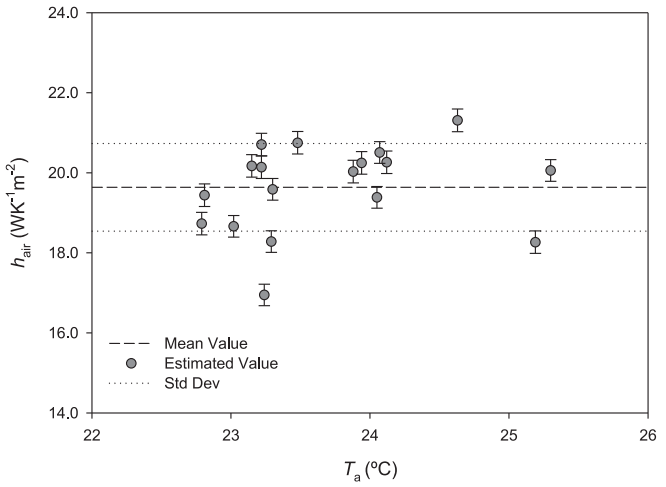

Fig. 10. Estimated heat transport coefficient for air during the cooling processes.

ing process in our experiments. Results are shown in Fig. 10, where the values are represented versus the ambient temperature.

A mean value of 19.6 WK^{-1}m^{-2} with a standard deviation of 1.1 was obtained for the combined heat transfer coefficient. According to Eq. (18), as the emissivity values can vary between 0 and 1, it would lead to a maximum value around 8 WK^{-1}m^{-2} for h_r in our experiments, and thus to convection heat transfer coefficients of air around 12 W K^{-1}m^{-2}. Typical values of the convective heat transfer coefficient for air in free convection are in the interval 2.5–25 WK^{-1} m^{-2} [36].

4. Conclusion

Through-plane thermal conductivity of different polymeric ion-exchange membranes have been estimated using a simple Leeś disc method. The found values varied between 0.03 and 0.41 WK^{-1} m^{-1}, depending on the membrane structure and composition, which agree with the thermal conductivity values of typical polymers.

The value of the thermal conductivity depended mainly of the membrane composition and no significant correlation was observed between thermal conductivity and membrane ion-exchange capacity for homogeneous and reinforced membranes. A positive correlation was observed for heterogeneous membranes, but the different physical properties of the membranes have made conclusive analysis on a direct correlation impossible. Lower values were obtained, in general, for tested reinforced membranes. For Nafion 1100 EW series of membranes tested, a correlation was observed between thermal conductivity and thickness suggesting the existence of a size effect on the through-plane thermal conductivity.

Thermal resistance of the membranes was also estimated. In general, denser homogeneous membranes showed lower values.

The values estimated for thermal conductivity of the tested membranes were in agreement with values reported in the literature, indicating that the method, despite its simplicity, can be useful for estimating through-plane thermal conductivity of thin polymeric ion-exchange membranes.

Declaration of Competing Interest

The authors declare that they have no known competing financial interests or personal relationships that could have appeared to influence the work reported in this paper.

CRediT authorship contribution statement

V.M. Barragán: Conceptualization, Methodology, Validation, Formal analysis, Investigation, Resources, Writing – original draft, Writing – review & editing, Visualization, Funding acquisition. **J.C. Maroto:** Validation, Formal analysis, Writing – review & editing, Visualization. **E. Pastuschuk:** Formal analysis, Writing – review & editing, Visualization. **S. Muñoz:** Methodology, Validation, Writing – review & editing, Visualization.

Acknowledgments

Financial support of this work by Banco de Santander and Universidad Complutense de Madrid within the frameworks of Projects PR26/16-20296 and PR75/18-21589 is gratefully acknowledged.

References

[1] Y. Wang, F. D, Ruiz Diaz, K.S. Chen, Z. Wang, X. Cordobes Adroher, Materials, technological status, and fundamentals of PEM fuel cells-a review, Mater. Today 32 (2020) 178–293, doi:10.1016/j.mattod.2019.06.005.
[2] Y. Mei, C.Y. Tang, Recent developments and future perspectives of reverse electrodialysis technology: a review, Desalination 425 (2018) 156–174, doi:10.1016/j.desal.2017.10.021.
[3] V.M. Barragán, K.R. Kristiansen, S. Kjelstrup, Perspectives on thermoelectric energy conversion in ion-exchange membranes, Entropy 20 (2018) 905, doi:10.3390/e20120905.
[4] M. Khandelwal, M.M. Mench, Direct measurement of through-plane thermal conductivity and contact resistance in fuel cell materials, J. Power Sources 161 (2006) 1106–1115, doi:10.1016/j.jpowsour.2006.06.092.
[5] O. Burheim, H. Su, S. Pasupathi, J.G. Pharoah, B.G. Pollet, Thermal conductivity and temperature profiles of the micro porous layers used for the polymer electrolyte membrane fuel cell, Int. J. Hydrogen Energy 38 (2013) 8437–8447, doi:10.1016/j.ijhydene.2013.04.140.
[6] N. Alhazmi, D.B. Ingham, M.S. Ismail, K. Hughes, L. Ma, M. Pourkashanian, The through-plane thermal conductivity and the contact resistance of the components of the membrane electrode assembly and gas diffusion layer in proton exchange membrane fuel cells, J. Power Sources 270 (2014) 59–67, doi:10.1016/j.jpowsour.2014.07.082.
[7] K.R. Kristiansen, V.M. Barragán, S. Kjelstrup, Thermoelectric power in ion exchange membrane cells relevant to reverse electrodialysis plants, Phys. Rev. Appl. 11 (2019) 044037, doi:10.1103/PhysRevApplied.11.044037.
[8] K.D. Sandbakk, A. Bentien, S. Kjelstrup, Thermoelectric effects in ion conducting membranes and perspectives for thermoelectric energy conversion, J. Membr. Sci. 434 (2013) 10–17, doi:10.1016/j.memsci.2013.01.032.
[9] M. Jokinen, J.A. Manzanares, K. Kontturi, L. Murtomäki, Thermal potential of ion-exchange membranes and its application to thermoelectric power generation, J. Membr. Sci. 499 (2016) 234–244, doi:10.1016/j.memsci.2015.10.042.
[10] M. Ahadi, M. Andisheh-Tadbir, M. Tam, M. Bahrami, An improved transient plane source method for measuring thermal conductivity of thin films: deconvoluting thermal contact resistance, Int. J. Heat Mass Transf. 96 (2016) 371–380, doi:10.1016/j.ijheatmasstransfer.2016.01.037.
[11] O. Burheim, P.J.S. Vie, J.G. Pharoah, S. Kjelstrup, *Ex situ* measurements of through-plane thermal conductivities in a polymer electrolyte fuel cell, J. Power Sources. 195 (2010) 249–256, doi:10.1016/j.jpowsour.2009.06.077.
[12] R. Bock, H. Karoliussen, F. Seland, G. B, M.S.Thomassen Pollet, S. Holdcroft, O.S. Burheim, Measuring the thermal conductivity of membrane and porous transport layer in proton and anion exchange membrane water electrolyzers for temperature distribution modelling, Int. J. Hydrogen Energy 45 (2020) 1236–1254, doi:10.1016/j.ijhydene.2019.01.013.
[13] W.B. Chang, H. Fang, J. Liu, C.M. Evans, B. Russ, B.C. Popere, S.N. Patel, M.L. Chabinyc, R.A. Segalman, Electrochemical effects in thermoelectric polymers, ACS Macro Lett. 5 (2016) 455–459, doi:10.1021/acsmacrolet.6b00054.
[14] C. Huang, X. Qian, R. Yang, Thermal conductivity of polymers and polymer nanocomposites, Mater. Sci. Eng. 132 (2018) 1–22, doi:10.1016/j.mser.2018.06.002.
[15] L. Zhang, H. Deng, Q. Fu, Recent progress on thermal conductive and electrical insulating polymer composites, Compos. Commun. 8 (2018) 74–82, doi:10.1016/j.coco.2017.11.004.
[16] H. Naseem, H. Murthy, A simple thermal diffusivity measurement technique for polymers and particulate composites, Int. J. Heat Mass Transf. 137 (2019) 968–978, doi:10.1016/j.ijheatmasstransfer.2019.03.171.
[17] H. Chen, V.V. Ginzburg, J. Yang, Y. Yang, W. Liu, Y. Huang, L. Du, B. Che, Thermal conductivity of polymer-based composites: fundamental and applications, Prog. Polym. Sci. 59 (2016) 41–85, doi:10.1016/j.progpolymsci.2016.03.001.
[18] N. Burger, A. Laachachi, M. Ferriol, M. Lutz, V. Toniazzo, D. Ruch, Review of thermal conductivity in composites: mechanisms, parameters and theory, Prog. Polym. Sci. 61 (2016) 1–28, doi:10.1016/j.progpolymsci.2016.05.001.
[19] R.C. Kerschbaumer, S. Stieger, M. Gschwandl, T. Hutterer, M. Fasching, B. Lechner, L. Meinhart, J. Hildenbrandt, B. Schrittesser, P.F. Fuchs, G.R. Berger,

W. Friesenbichler, Comparison of steady-state and transient thermal conductivity testing methods using different industrial rubber compounds, Polym. Test. 80 (2019) 106121, doi:10.1016/j.polymertesting.2019.106121.
[20] J. Vanneste, J.A. Bush, K.L. Hickenbottom, C.A. Marks, D. Jassby, C.S. Turchi, T.Y. Cath, Novel thermal efficiency-based model for determination of thermal conductivity of membrane distillation membranes, J. Membr. Sci. 548 (2018) 293–308, doi:10.1016/j.memsci.2017.11.028.
[21] G. Unsworth, N. Zamel, X. Li, Through-plane thermal conductivity of the microporous layer in a polymer electrolyte membrane fuel cell, Int. J. Hydrogen Energy 37 (2012) 5161–5169, doi:10.1016/j.ijhydene.2011.12.012.
[22] M. Monde, Analytical method in inverse heat transfer problem using laplace transform technique, Int. J. Heat Mass Transf. 43 (2000) 3965–3975, doi:10.1016/S0017-9310(00)00040-5.
[23] B. Blackwell, J.V. Beck, A technique for uncertainty analysis for inverse heat conduction problems, Int. J. Heat Mass Transf. 53 (2010) 753–759, doi:10.1016/j.ijheatmasstransfer.2009.10.014.
[24] V.M. Barragán, M.A. Izquierdo-Gil, J.C. Maroto, P. Antoranz, S. Muñoz, Estimation of the through-plane thermal conductivity of polymeric ion-exchange membranes using finite element technique, Int. J. Heat Mass Transf. 176 (2021) 121469, doi:10.1016/j.ijheatmasstrnsfer.2021.121469.
[25] P. Philip, L. Fagbenle, Design of Leeś disc electrical method for determining thermal conductivity of a poor conductor in the form of a flat disc, IJSRIS 9 (2) (2014) 335–343.
[26] N. Sombatsompop, A.K. Wood, Measurement of thermal conductivity of polymers using an improved Leeś disc apparatus, Polym. Test. 16 (1997) 203–223, doi:10.1016/S0142-9418(96)00043-8.
[27] H.C. Aristide, F.J.L. Comlan, G.V. Bertrand, D. Armand, A. Malahimi, V. Antoine, Assessment of the thermal conductivity of local building materials using Leeś disc and hot strip devices, Asian J. Adv. Basic Sci. 7 (2) (2019) 5–13, doi:10.33980/ajabs.2019.v07i02.002.
[28] Y.A. Çengel, A.J. Ghajar, Heat and Mass Transfer, Fundamental & Applications, Mc Graw Hill, Singapore, 2015.
[29] A.J. Chapman, Heat Transfer, The Macmillan Company, 1960 New York.
[30] C.I. Idumah, A. Hassan, Recently emerging trends in thermal conductivity of polymer nanocomposites, Rev. Chem. Eng. 32 (2016) 413–457, doi:10.1515/revce-2016-0004.
[31] B. Dogan, H. Tan, The numerical and experimental investigation of the change of the thermal conductivity of expanded polystyrene at different temperatures and densities, Int. J. Polym. Sci. (2019) 6350326 2019, doi:10.11155/2019/6350326.
[32] C.L. Choy, Y.W. Wong, G.W. Yang, T. Kanamoto, Elastic modulus and thermal conductivity of ultra drawn polyethylene, J. Polym. Sci. Part B Polym. Phys. 37 (1999) 33593367, doi:10.1002/(SICI)1099-0488(19991201)37:23(3359::AID-POLB11)3.0.CO;2-S.
[33] T. Feng, J. He, A. Rai, D. Hun, J. Liu, S.S. Shrestha, Size effect in the thermal conductivity of amorphous polymers, Phys. Rev. Appl. 14 (2020) 044023 1, doi:10.1103/PhysRevApplied.14.044023.
[34] S. Slade, S.A. Campbell, T.R. Ralph, F.C. Walsh, Ionic conductivity of an extruded Nafion 1100 EW series of membranes, J. Electrochem. Soc. 149 (2002) A1556–A1564 10.1149/1.1517281.
[35] R.H. Tarkhanyan, D.G. Niarchos, Reduction in lattice thermal conductivity of porous materials due to inhomogeneous porosity, Int. J. Therm. Sci. 67 (2013) 107–112, doi:10.1016/j.ijthermalsci.2012.12.008.
[36] P. Kosky, R. Balmer, W. Keat, G. Wise, Exploring Engineering. An Introduction to Engineering and Design, Academic Press, Amsterdam, 2012 third ed..